European Journal of Technique

journal homepage: https://dergipark.org.tr/en/pub/ejt

Vol. 13, No. 1, 2023

Assessment of Risky Buildings according to the Regulation for Determination of Risky Buildings (RDRB 2019): The Case of Şanlıurfa

İsmail Ümit ÇIKMAN[1*], Mehmet Emin Öncü[2], Şermin KOÇYİĞİT[3]

[1*]Dicle University, Technical Sciences Vocational School, Diyarbakır,Türkiye. (e-mail: umit.cikman@dicle.edu.tr).
[2] Dicle University, Civil engineering Department, Diyarbakır, Türkiye. (e-mail: oncume@dicle.edu.tr).
[3] Dicle University, Technical Sciences Vocational School, Diyarbakır,Türkiye.(e-mail: sermin.kocyigit@dicle.edu.tr).

ARTICLE INFO

Received: Oct., 10. 2022
Revised: Feb, 03. 2023
Accepted: Feb, 27. 2023

Keywords:
Risky buildings
RDRB
Earthquake
Risk assessment

Corresponding author: *İsmail Ümit ÇIKMAN*

ISSN: *2536-5010* | e-ISSN: *2536-5134*

DOI: https://doi.org/10.36222/ejt.1187068

ABSTRACT

The majority of risky structures in Türkiye's building stock were constructed before 2000. It has been discovered that buildings constructed before the year 2000 lack engineering services and cannot fulfill the requirements of current regulations. Buildings constructed before 2000 are clearly incapable of providing the required performance and ductility in the event of an earthquake. Therefore, based on the Regulation for Determination of Risky Buildings (RDRB 2019), field studies were conducted on existing buildings built before 2000 in the Siverek district of Şanlıurfa. a two-stories reinforced concrete building designed in accordance with field study data was analyzed by following the risk analysis stages for low-rise reinforced concrete buildings in RDRB 2019. An elemental risk analysis was performed on 16 columns, which are vertical elements of the structure, and then a floor-based risk assessment was performed. As a consequence, it was concluded that the building designed in accordance with condition before 2000 was at risk.

1. INTRODUCTION

Türkiye is located in an active earthquake zone due to its geographical position. Since there are no ways for determining the precise time of earthquakes, our country will inevitably be impacted by natural disasters such as earthquakes, together with considerable loss of life and property. Türkiye is located on active fault zones such as the East Anatolian Fault (EAF), the North Anatolian Fault (NAF) and the Anatolian-Aegean Subduction Zone (AASZ) [1]. The Pacific Seismic Belt accounts for 81% of all earthquakes in the world, whereas the Alpine-Himalayan Seismic Belt accounts for 17% [2]. Because of its position, Türkiye is located on the Alpine-Himalayan Seismic Belt. The Earthquake Zones Map reveals that 92% of our country is in earthquake zones, 95% of our population lives with earthquake risk, 98% of large-scale industrial enterprises, and 93% of our dams are located in earthquake risk areas [3]. As a result of the major earthquakes that took place in our country, it has been shown that existing buildings in the regions are highly vulnerable to earthquake risk. [4] As a result, conducting risk assessments rapidly and efficiently is critical in order to figure out how this unsafe building stock might react to earthquakes. Otherwise, more catastrophic loss of life and property would be inevitable. Regulation for Determination of Risky Buildings (RDRB), which were initially published in 2013 and whose final version came into force in 2019, should be thoroughly investigated in this context, and existing building stocks should be evaluated within the scope of this regulation. Recent studies on this subject can be listed as follows. Ayhan and at all [5] made a risk assessment in the city center of Siirt and calculated the building performance scores in the light of the information obtained from 5 buildings whose demolition decision was taken by the administration. Considering the performance scores obtained for the 5 structures, they found that there was a 25 base score between the lowest and highest scores. The scores of the 2 buildings were the same, and the obtained scores determined that there was an important preliminary study in determining the risk priority in the buildings. Türkoglu and Atalay Meydanli [6] evaluated the seismic performance of Piyalepasa Mansion in Eregli as an example in their study. They created a three-dimensional analytical model of the building according to the measurements and observations made in situ. Considering the earthquake parameters selected specifically for the location of the building, the calculation methods defined in the regulations were applied. In the analyzes made, displacements and internal forces caused by the structure's own weight and earthquake forces were determined and compared the earthquake safety of the building determined according to both regulations (RYTEIE and TBDY). In his study, Alicioglu [7] examined the buildings in Yunusemre and Sehzadeler districts of Manisa province according to RYTEIE. In the field studies of risky building detection, it has been determined that most of the building stock in the districts consists of reinforced concrete buildings built in 2000 and before. In line with the data obtained by examining the concrete compressive strengths, reinforcement classes, reinforcement layouts, column sizes and floor plans of 325 existing reinforced concrete buildings in the city center of Manisa, which were built between 1957 and 2001 within the scope of urban transformation, a prototype building representing the buildings in the city center of Manisa was created. He has determined the risk situations by conducting a survey of the prototype building and the buildings that have not been identified as risky buildings. With the risk assessment made for the prototype building, it has been determined that the existing reinforced concrete buildings with two or more floors carry earthquake risk. Turkel and Tekeli [8] made a risk assessment of 100 existing reinforced concrete residential buildings according to RYTEIE. The x and y directions of the buildings were analyzed with Sta4-Cad v.13, a ready-made package program used in the market. They envisaged five different material classes for each existing building: A, B, C, D and E. A total of 1000 buildings were analyzed. They determined the effectiveness of material properties in the risk assessment of reinforced concrete buildings. In addition, suggestions were made for risk assessment without the need for structural modeling and computer analysis. Using the Idecad software, Altın Karayahşi [9] investigated the earthquake resistance of 15 public buildings. Linear Performance Analysis and Risky Structure Analysis were used in the models under the impact of a four-way earthquake and found that the results in both analysis methods were similar. Korkmaz [10] carried out a risk analysis of a four-stories reinforced concrete structure using the Japanese Seismic Index Method (JSIM) and the RDRB 2013. The results of the two methods were compared, and similar and different sections were identified. The causes of the similarities and differences are discussed. Finally, Altın Karayahşi emphasized that the Japanese Seismic Index Method (JSIM) may be used in our country as well. Okuyucu and at all [11]. A total of 1194 reinforced concrete structures in the Palandoken district of Erzurum were examined, and as 18 of the structures had 8 floors or more, they were excluded from the scope of RYTEIE during the risk assessment phase. As a result of the statistical analysis of the building performance scores, the buildings were distributed to 5 different risk groups. They concluded that, according to RYTEIE, 7.2% of the 1177 reinforced concrete structures evaluated were high risk, 62.4% moderate risk, 7.3% low risk, 22% safe and 0.7% very safe. Ekinci [12] investigated an eight-stories building built in 1984 in Ankara using RDRB 2013. Ekinci conducted the benefit-cost analysis of the building based on urban transformation principles, and as a consequence of the analysis, it was decided to reconstruct the building, despite the fact that retrofitting was more cost-effective than rebuilding. In a study, Can [13] described the FEMA 310, ATC-21 (Rapid Visual Screening of Building for Potential Seismic Hazards), and Japanese Seismic Index Method (JSIM), all of which are rapid assessment methods, in general. On the other hand, Can thoroughly review the RDRB and the Earthquake Screening Method (ESM), and examined the results by taking into account a total of 20 risky and 2 risk-free buildings, including thirteen buildings constructed before 1975 and 7 buildings after 1975 according to RDRB, based on ESM. As a consequence, it can be determined that both methods produced similar results for reinforced concrete structures up to six-stories and that the ESM was more cost and time efficient. It can also be emphasized that, as a result of the preliminary work with the ESM, safe buildings would be separated and risky buildings would be prioritized. Isik and Tozlu [14] selected the ground classes, carrier system type and apparent building quality parameters of an existing five-storey reinforced concrete building as variables by using the first stage evaluation method, which is included in the principles regarding the identification of risky structures that entered into force in 2013 and according to these variables. Calculated building performance scores. They compared the calculated performance scores and interpreted the effects of the selected variables on the building performance scores. In their post-earthquake damage assessment studies on a building built in Kadıköy District of Istanbul Province in 1991, Hacımustafaoğlu et al., [15] used the rapid screening method and made observational analysis. As a consequence, they determined that the rapid screening method may be used in the identification of risky buildings in post-earthquake damage assessment studies, leading to fast and cost-effective identification. Gürbüz and Tekin [16] emphasized the necessity of determining the risk status of existing buildings in order to be prepared for an earthquake. In this framework, they calculated the performance scoring based on an imagined region on the map, in accordance with the regulation on the “Methods that Can Be Used to Determine the Regional Earthquake Risk Distribution of Buildings,” which came into effect in 2013. Işık [17] compared the conditions that appeared utilizing the Japanese Seismic Index, Canadian Seismic Screening, and P25 Rapid Assessment methods to a school building that was entirely demolished in the 2011 Van earthquake. Işık and Tozlu [18] calculated the performance score and current status of an existing five-stories reinforced concrete structure based on the 1st Stage Assessment Method within the scope of RDRB, which went into effect in 2013. Risk analysis was carried out in the Siverek district of Şanlıurfa in this study. A low-rise reinforced concrete building was designed based on the average values obtained from the buildings. Following that, a risk assessment was done in accordance with the RDRB 2019, and the steps to be followed in risk assessment were thoroughly examined.

2. MATERIAL AND METHOD

The designed building was examined as a result of field investigations on existing buildings constructed before 2000 in the Siverek district of Şanlıurfa. The designed building comprises two stories and has a reinforced concrete frame system. The risk analysis was carried out in accordance with the steps determined for low-rise reinforced concrete buildings based on RYTEIE 2019. The risk assessment of the columns, which are represented as vertical elements, was completed first, followed by the risk assessment of the building on a floor-by-floor basis, in accordance with the obtained data and the analysis steps determined in RYTEIE 2019. If any floor was determined to be risky, the whole building was considered as risky.

2.1. General Information on the Inspected Building:

Table 1 shows general information about the building to be designed. A risk structure analysis was done based on the static project.

TABLE I
GENERAL INFORMATION OF THE DESIGNED BUILDING

Map Spectral Acceleration Coefficients	SS = 0.386 S1 = 0.135
Local Soil Class	ZA
Soil Bearing Coefficient	Ks=4000t/m^3
Local Site Effect Coefficients	Fs = 0.800 F1 = 0.800
Design Spectral Acceleration Coefficients	SDS=SS×FS=0.386×0.800=0.309 SD1=S1×F1=0.135×0.800=0.108

For the building to be designed, the floor to be examined was assigned as the ground floor, and a survey was done on this floor. Another parameter, the carrier system knowledge level, was determined as a comprehensive knowledge level. The survey of the inspected building was carried out using various measuring devices, and Figures 1(a), (b), (c), and (d) show images of the survey processes.

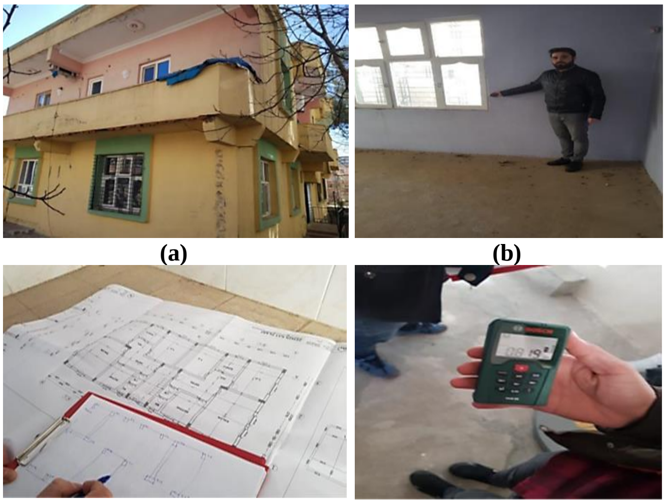

(a) **(b)** **(c)** **(d)**

Figure 1. Images of the survey process

To determine the reinforcements of the inspected building, X-ray scanning, a non-destructive method, was performed on six of the existing columns, and the reinforcement arrangement was determined by scratching half of these columns. Table 2 shows the identified reinforcements. Furthermore, the building's beams were 20 x 20 cm in size, and the reinforcements were 4 Ø 12 mm and Ø 8/25 mm, respectively.

TABLE 2.
COLUMN REINFORCEMENT RATIOS

Floor	No	Size (cm)	Longitudinal reinforcement (mm)	Stirrup (mm)	Compression	Corrosion
Ground	1	30X30	8 Ø 14	Ø 8/25	Non	Non
Ground	3	30X30	8 Ø 14	Ø 8/25	Non	Non
Ground	7	30X30	8 Ø 14	Ø 8/25	Non	Non

In order to determine the existing concrete strength of the building in Figure 2, a test hammer reading, which is a non-destructive examination method, was done from 8 different columns and concrete sampling was performed from 4 columns in Figure 3. Table 3 also shows the values of the core samples collected.

TABLE 3.
CORE VALUES OF THE BUILDING

Sample Name	Floor Location	Core Values (MPa)
Core 1	Ground Floor	7.84 MPa
Core 2	Ground Floor	7.35 MPa
Core 3	Ground Floor	6.69 MPa
Core 4	Ground Floor	7.54 MPa
Arithmetic Mean		7.36 MPa
Reduction Parameter (RDRB 4.1.11)		0.85
Conversion parameter mean current concrete value to be taken as Compressive Strength		6.63 MPa

Figure 2. Non-destructive examination method

Figure 3. Coring process

The calculation steps given in Table 4 were used for the analysis process of the designed building. Ecm: Existing concrete modulus of elasticity, (EI)e: Effective flexural stiffness, (EcmI)o: Flexural stiffness of gross section, fcm: Existing concrete compressive strength, Gcm: Existing concrete shear modulus.

TABLE 4.
CALCULATION STEPS TO BE USED FOR THE ANALYSIS

Effective bending stiffnesses	In beams: $(EI)e=0.3(EcmI)_0$ In columns: $(EI)e=0.5(EcmI)_0$
Concrete modulus of elasticity	$E_{cm}=5000\sqrt{fcm}=5000\sqrt{6.63}=12874.393$ MPa
Shear modulus	$G_{cm}=0.4Ecm=0.4x12874.393=5149.757$ MPa
The reinforcement class was determined as S220 for transverse and longitudinal reinforcements.	

Figures 4a and 4b show the identification of the reinforcement diameter with a calliper and the identification of stirrup spacing with a tape measure on the scratched columns.

(a) **(b)**

Figures 4a and 4b. Images of the reinforcement identification processes

Figure 5 shows a three-dimensional view of a structure designed by us that is not exactly the same size and dimensions as the average values obtained.

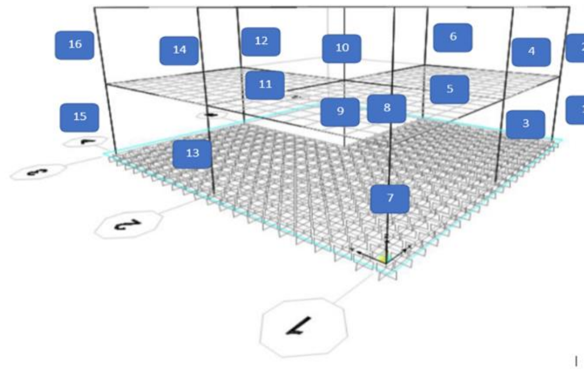

Figure 5. 3D view of the building with risk assessment

2.1.1. Risk Assessment of Colon No: 1

While identifying the risky building, the risk of the elements should be assessed first. The risk of the columns, which are expressed as vertical elements, was assessed for this purpose. As seen in column no:1, risk situations of the elements were calculated one by one. The examination steps are mentioned in the details below in this context.

Column (Ground Floor):
Axial Load Calculation:
The axial load of the column was obtained under (G+nQ+Ex/6) loading.
Nk: Column axial force obtained under vertical loads and reduced earthquake effects
n: 0.3 (live load reduction factor)
G (Dead load impact) = -66.684 kN,
Q (Live load impact) = -22.750 kN
Ex (Earthquake load effect) = -41.775 kN
Nk (G+nQ+Ex/6) = -80.427 kN

Calculation of Column Moments:
Internal forces were obtained under (G+0.3Q+Ex) loading at the upper and lower ends of the column.

Upper:

G_{22} = -7.455 kNm, G_{33} = -6.849 kNm
Q_{22} = -2.132 kNm, Q_{33} = -1.954 kNm
Ex_{22} = -1.319 kNm, Ex_{33} = -40.688 kNm
M_{22e} = (-7.455) + 0.3*(-2.132) + (-1.319) = -9.414 kNm
M_{33e} = (-6.849) + 0.3*(-1.954) + (-40.688) = -48.123 kNm
M_{22e}: (Column/wall moment around 2-2 axis under vertical loads and earthquake effects)
M_{33e}: (Column/wall moment around 3-3 axis under vertical loads and earthquake effects)

Lower:

G_{22} = 3.731 kNm, G_{33} = 3.344 kNm
Q_{22} = 1.060 kNm, Q_{33} = 0.961 kNm
Ex_{22} = -1.180 kNm, Ex_{33} = 113.171 kNm
M_{22e} = (3.731) + 0.3*(1.060) + (-1.180) = 2.869 kNm
M_{33e} = (3.344) + 0.3*(0.961) + (113.171) = 116.803 kNm

2.1.2. Calculation of Column Moment Capacities:

For the calculation of the moment capacities in the columns, firstly, the ratio of the internal forces obtained above to each other and the slopes of the lines for the upper and lower were found. The raw values of the capacity moments obtained under certain axial load values were then obtained. M_{22} and M_{33} capacity moments were determined for every 15 degrees between 0 and 90 degrees by interpolating based on the raw values obtained and the axial load (Nk) value we found. Table 5 shows the determined values, which were used to create an interaction diagram. Figure 6 shows the effect diagram. The coordinates of the intersections of the diagram and the lines give the column/wall plastic moments M_{22p} and M_{33p}.

Upper:

$$\tan\theta_d = M_{22}/M_{33} = -9.414/-48.123 = 0.1956$$

Lower:

$$\tan\theta_d = M_{22}/M_{33} = 2.896/116.803 = 0.0246$$

Table 5. M_{22p} and M_{33p} values corresponding to axial force for column no: 1

P	M_{33} 0°	M_{33} 15°	M_{33} 30°	M_{33} 45°	M_{33} 60°	M_{33} 75°	M_{33} 90°
80.472	39.718	37.756	33.332	25.491	16.626	7.436	0
P	M_{22} 0°	M_{22} 15°	M_{22} 30°	M_{22} 45°	M_{22} 60°	M_{22} 75°	M_{22} 90°
80.472	0	7.436	16.626	25.491	33.332	37.756	39.718

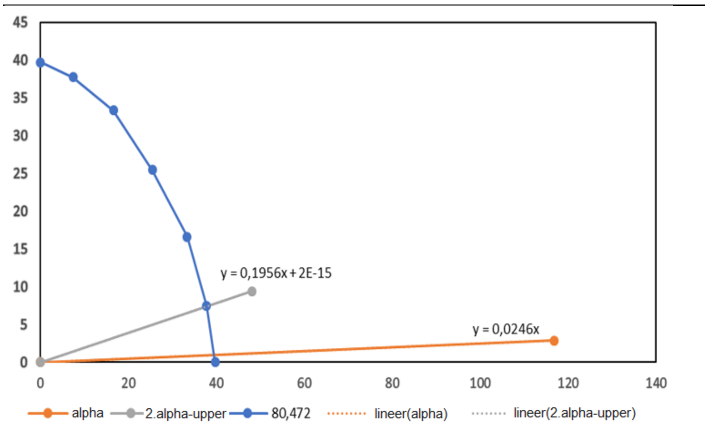

Figure 6. M_{22}-M_{33} interaction diagram for column no: 1

Upper	**Lower**
M_{22p} = -7.388 kNm	M_{22p} = 0.971 kNm
M_{33p} = -37.769 kNm	M_{33p} = 39.462 kNm

The Ve (Shear force calculated under vertical loads and earthquake effects) Calculation:

The shear force value was found as below by writing in situ in the combination of the internal forces (G+0.3Q+Ex/2) obtained.
G_{22} = -3.397 kN, G_{33} = -3.729 kN,
Q_{22} = -0.972 kN, Q_{33} = -1.064 kN
Ex_{22} = -51.286 kN, Ex_{33} = -0.047 kN
V_{22e} = (-3.397) + 0.3*(-0.972) + (-51.286/2) = -29.332 kN
V_{33e} = (-3.729) + 0.3*(-1.064) + (-0.047/2) = -4.072 kN

The Vr (Shear force of column, beam or wall section) Calculation:

$f_{ctm} = 0.35\sqrt{6.63} = 0.90$ MPa, $f_{ywm} = 220$ MPa, $c_c = 20$ mm, $A_{s22} = 151$ mm^2, $A_{s33} = 151$ mm^2
$S_{22} = S_{33} = 250$ mm (orta), b = 300 mm, $h_l = 300$ mm

(f_{ctm}: Existing concrete tensile strength, As: area of transverse reinforcement, fywm: Current yield strength of transverse reinforcement, Cc: Distance from the outer surface of the element to the outermost centre of longitudinal reinforcement, s: Spacing of transverse reinforcement, hı: Element length in 2-2 direction, b: element length in the 3-3 direction)

$\zeta = 1+0.07\, N_K/A_c$: column under compressive force (ζ: Column axial force factor)
$\zeta = 1+0.07\, N_K/A_c$: column under tensile force (A_c : Gross column cross-sectional area)

$$V_{22U} = 0.5 f_{ctm} b (h_\iota - c_c)\zeta + A_{s22} f_{ywm} \frac{(h\iota - cc)}{s22} + V_{manto} \le 0.22 f_{cm} b h_\iota$$

$$V_{33U} = 0.5 f_{ctm} h_\iota (b - c_c)\zeta + A_{s33} f_{ywm} \frac{(h\iota - cc)}{s33} + V_{manto} \le 0.22 f_{cm} b h_\iota$$

V_u: Uniaxial column/wall shear capacity

$0.22\, f_{cm} b h_\iota = 131.274$ kN

$$V_{22u} = 0.5 * 0.90 * 300 * 280 * (1 + 0.07 * 80.472/90) + 151 * 220 * 280/250 = 77.372kN \le 131.274kN$$

$$V_{33u} = 0.5 * 0.90 * 300 * 280 * (1 + 0.07 * 80.472/90) + 151 * 220 * 280/250 = 77.372kN \le 131.274kN$$

V_{33u}=0.5*0.90*300*280*(1+0.07*80.472/90)+151*220*280/

250 = 77.372 kN ≤ 131.274 kN

$$V_r = V_{22u} V_{33u} = \sqrt{\frac{(V_{22e})^2 + (V_{33e})^2}{(V_{33u} V_{22e})^2 + (V_{33e} V_{22u})^2}}$$

$$V_r = 77.372 * 77.372 \sqrt{\frac{(-29.332)^2 + (-4.072)^2}{(77.372*(-29.332))^2 + (-4.072*77.372)^2}} = 77.372kN$$

2.1.3. Ve Calculation (BA (Beam articulation) / CA (Column articulation) analysis):

In order to determine the beam articulation or column articulation in the column, first of all, the beam moments, M_{aki} values and directions of the beams connected to the column, calculated under 1.4G+1.6Q loading, were determined. The direction of the earthquake effect, Ex at that end of the beam is determined; if both are in the same direction, the plastic end moment of the beam can be taken $M_{pki} = M_{aki}$, but if they are in opposite directions, $M_{pki}=M_{aki}/3$. Then, M_{pkx} and M_{pky} values are determined, respectively, and then M_{pk22} and M_{pk33} values are determined according to the angle value.

Upper

$$M_{ak1} = -12.504kNm, \quad Ex \Rightarrow M_{pk1} = -12.504kNm$$

$$M_{ak2} = -14.153kNm, \quad Ex \Rightarrow M_{pk2} = -4.718kNm$$

$$M_{pkx} = -12.504kNm, \; M_{pky} = -4.718kNm$$

$$M_{pk22} = M_{pkx} \cos\theta - M_{pky} \sin\theta,$$

$$M_{pk22} = (-12.504)\cos 0 - (-4.718)\sin 0 = -12.504kNm$$

$$M_{pk33} = M_{pkx} \sin\theta + M_{pky} \cos\theta,$$

$$M_{pk33} = (-12.504)\sin 0 + (-4.718)\cos 0 = -4.718kNm$$

After these processes, the lower column upper-end moments and the upper column lower-end moments of the columns connected to the junction area are determined under the effect of the earthquake (Ex); then, the column/wall moment M_{22k} and M_{33k} values around the 2-2 and 3-3 axis transferred to the column/wall by the plastic articulation of the beams are obtained.

$$M_{22}^{upper} = -1.319kNm, \; M_{33}^{upper} = -40.688kNm,$$

$$M_{22}^{lower} = 4.435kNm, \; M_{33}^{lower} = 26.358kNm,$$

$$M_{22k} = M_{pk22} = \frac{\left|M_{22}^{upper}\right|}{\left|M_{22}^{üst}\right| + \left|M_{22}^{lower}\right|},$$

$$M_{22k} = -(-12.504)\frac{1.319}{1.319+4.435} = 2.866kNm$$

$$M_{33k} = M_{pk33} \frac{\left|M_{33}^{upper}\right|}{\left|M_{33}^{üst}\right| + \left|M_{33}^{lower}\right|},$$

$$M_{33k} = -4.718 \frac{40.688}{40.688+26.358} = -2.863kNm$$

Lower

Since there is a foundation connection and there is no beam, M_{22k} and M_{33k} values will be taken as M_{22p} and M_{33p} values.

$$M_{22k} = 0.971kNm$$
$$M_{33k} = 39.462kNm$$

The M_{22k} and M_{33k} values for the upper and lower ends are placed in the interaction diagram. Figure 7 shows the interaction diagram. If the values remain inside the diagram, beam articulation (BA) is identified; otherwise, column articulation (CA) is identified. As a result, if the BA condition is determined, the column end moments M_{22k} and M_{33k} will be used in the calculation, and if the CA condition is determined, the M_{22p} and M_{33p} values will be used in the calculation. Critical end moments of the upper and lower ends chosen based on the BA or CA status determined at the lower and upper ends, will be taken as $M_{22kr}{}^{upper}$, $M_{33kr}{}^{upper}$, $M_{22kr}{}^{lower}$, $M_{33kr}{}^{lower}$, respectively.

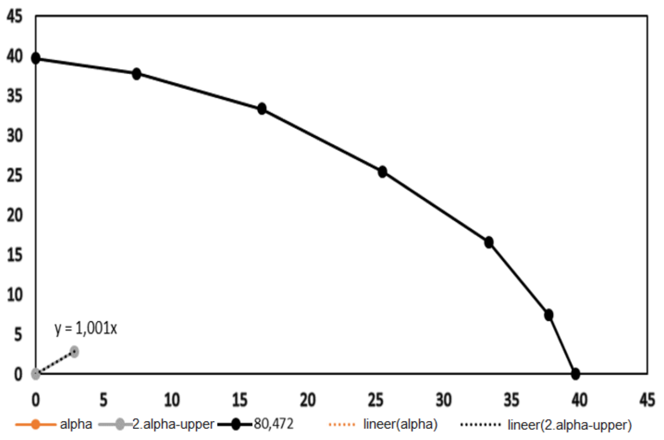

Figure 7. BA and CA status in M_{22} and M_{33} interaction diagram for column no: 1

M22k and M33k values at the upper and lower ends of the column were obtained as follows.

Upper End $M_{22k} = 2.866kNm$ $\quad M_{22p} = 20.794kNm$

$M_{33k} = -2.863kNm$

Lower End $M_{22k} = 0.971kNm$ $\quad M_{22p} = 0.971kNm$

$M_{33k} = 39.462kNm$

By comparing the M_{22k} and M_{22p} values obtained for the upper end of the column, it was determined whether the BA or CA was determined. Since there is no beam at the lower end, the CA situation was directly examined.

Upper End

$$M_{22p} = 20.794kNm > M_{22k} = 2.866kNm(BA)$$

Lower End Kiriş bulunmamaktadır. **(CA)**

$$M_{22kr}^{upper} = 2.866kNm, \qquad V_{22e} = \frac{\left|M33_{kr}^{upper}\right| + \left|M33_{kr}^{lower}\right|}{\ell n}$$

$$M_{33kr}^{upper} = -2.863kNm, \qquad V_{33e} = \frac{\left|M22_{kr}^{upper}\right| + \left|M22_{kr}^{lower}\right|}{\ell n}$$

$$M_{22kr}^{lower} = 0.971kNm,$$

$$M_{33kr}^{lower} = 39.462kNm,$$

ℓn: Beam net length or column net length

Critical end moments of selected upper and lower ends were respectively M_{22kr} ^{upper}, M_{33kr} ^{upper}, M_{22kr} ^{lower}, and M_{33kr} ^{lower} as above.

$$V_{22e} = \frac{2.863+39.462}{2.8} = 15.116kN$$

$$V_{33e} = \frac{2..866+0.971}{2.8} = 1.370kN$$

Vr Calculation (BA/CA Analysis):

$$f_{ctm} = 0.35\sqrt{6.63} = 0.90\ MPa,\ f_{ywm} = 220MPa,\ c_c = 20mm$$

$$A_{s22} = 151mm^2,\ A_{s33} = 151mm^2,$$

$$s_{22} = s_{33} = 250mm\ (middle), b = 300mm, h_1 = 300mm$$

$\zeta = 1 + 0.07N_K / A_c$: under column compressive force

$\zeta = 1 + 0.07N_K / A_c$: under column tensile force

$$V_{22u} = 0.5 f_{ctm} b (h_1 - c_c)\zeta + A_{s22} f_{ywm} = \frac{(h_1 - c_c)}{s_{22}} + V_{manto} \le 0.22 f_{cm} bh_t$$

$$V_{33u} = 0.5 f_{ctm} h_t (b - c_c)\zeta + A_{s33} f_{ywm} = \frac{(h_1 - c_c)}{s_{33}} + V_{manto} \le 0.22 f_{cm} bh_t$$

$$0.22 f_{cm} bh_t = 0.22*6.63*300*300 = 131.274kN$$

$$V_{22u} = 0.5*0.90*300*280*(1+0.07*80.472/90) + 151*220*280/250 = 77.372kN \le 131.274kN$$

$$V_{33u} = 0.5*0.90*300*280*(1+0.07*80.472/90) + 151*220*280/250 = 77.372kN \le 131.274kN$$

$$V_r = V_{22u}V_{33u}\sqrt{\frac{(V_{22e})^2 + (V_{33e})^2}{(V_{33u}V_{22e})^2 + (V_{33e}V_{22u})^2}}$$

$$V_r = 77.372*77.372\sqrt{\frac{(-29.332)^2 + (-4.0.72)^2}{(77.372*(-29.332))^2 + (-4.072*77.372)^2}} = 77.372kN$$

In the above steps, Ve and Vr values were calculated for R analysis and BA/CA status, respectively. In the next step, in order to determine the Ve/Vr value, these two situations will be compared as stated below and the minimum values will be taken as a basis during the process.

Ve/Vr Calculation:

$$\frac{V_e}{V_r} = \sqrt{\frac{(V_{22e})^2 + (V_{33e})^2}{(V_{22r})^2 + (V_{33r})^2}}$$

$$R\ Analizi \rightarrow V_e = 29.332kN$$
$$V_r = 77.372kN$$

$$V_e/V_r = \frac{\sqrt{29.332^2 + 4.072^2}}{77.372} = 0.383$$

$$BA/CA \rightarrow V_e = 15.116kN$$
$$V_r = 77.372kN$$

$$V_e / V_r = \frac{\sqrt{15.116^2 + 1.370^2}}{77.372} = 0.196$$

$$V_e/V_r = Min(V_e/V_r) \Rightarrow \quad V_e/V_r = 0.196,\ V_e = 15.116kN,\ V_r = 77.372kN$$

2.1.4. Determination of Element Class:

The element class was selected by first identifying which section of the column classification table (RYTEIE 2019) would be inspected based on the Ve/Vr ratio. The element class was determined in the table for situations that meet the stirrup spacing, hook situation, and transverse reinforcement area requirements, as well as situations that do not.

$(A_{sh}/s_{bk})_{22} = 151/250/260 = 0.0023,$
$(A_{sh}/s_{bk})_{33} = 151/250/260 = 0.0023,$
$V_e/V_r = 0.196$
$S = 250mm \geq 100mm, 135°hook,$
$A_{sh}/s_{bk} * f_{ywm}/f_{cm} = 0.0023 * 220/6.63 = 0.076$

(A_{sh}: The sum of the projections of the cross-sectional area values of all stirrup arms and distance pieces in the column or wall head zone along the height corresponding to the transverse reinforcement spacing, s: Transverse reinforcement spacing, b_k: distance between the outermost transverse reinforcement axes)

Considering the above parameters, the element class was determined as B according to the column classification table (RYTEIE 2019).

2.1.4. Determination of Limit Values:

According to the column group that is suitable for the determined element class, limit values will be found for the columns from the limit value m_{limit} of the Impact/capacity ratio and limit value $(\delta/h)_{limit}$ of the effective relative stories drift ratio (RYTEIE 2019). Linear interpolation will be made for intermediate values.

$$Nk/(f_{cm}Ac) = 80.472/(6.63*0.09*1000) = 0.135,$$
$$A_{sh}/(s_{bk}) = 151/250/260 = 0.0023,$$
$$m_{sınır} = 2.878$$

The $(\delta/h)_{limit}$ was determined as 0.016.

<u>Determination of Risk Status:</u>

<u>Upper End</u>

Impact $\{M_{22} = -9.414kNm, M_{33} = -48.123kNm$
Capacity $\{M_{22} = -7.388kNm, M_{33} = -37.769kNm$

$M = 49.035kNm$
$M_p = 38.485kNm$

<u>Lower End</u>

Impact $\{M_{22} = 2.869kNm, M_{33} = 116.803kNm$
Capacity $\{M_{22} = 0.971kNm, M_{33} = 39.462kNm$

$M = 116.838kNm$
$M_p = 39.474kNm$

Upper End

$m = 49.035/38.485 = 1.274 < 2.878$

Lower End

$$m = 116.838/39.474 = 2.960 < 2.878(\delta/h) = 0.0645/3 = 0.0215 < 0.016$$

The m_{limit} and $(\delta/h)_{limit}$ values determined with the determined m and (δ/h) values are compared for the two ends of the column as stated above, and if any condition is exceeded, the **element** will be considered as **risky**. The risk conditions of the other columns were made according to the steps followed in above column no: 1, and all columns were found to be risky.

3. RISK ASSESSMENT OF THE BUILDING

The element risk assessment of the building designed by us was completed, and the ground and first floors were subjected to a risk assessment to review the building's risk assessment. Based on this, the variables required for the analyses were determined as below and the risk conditions of the floors were identified. Because any of the floors investigated poses a risk, the building is considered as risky.

3.1. Ground Floor Assessment:

Sum of the axial load obtained from G + nQ loading: 9250000 N
Total number of columns on the floor: 8
Total column area on the floor: (300*300*8) = 720000 mm^2
Total axial compressive stress: (925000/720000) = 1.285 Mpa
Average axial compressive stress: (1.285/8) = 0.161 Mpa
Floor shear force limit value: 0.35
The sum of the shear forces of the elements exceeding the risk limit: 438.349 kN
Total floor shear force: 438.349 kN
438.349/438.349 = 1 > 0.35 **The floor is risky**

3.2. 1st Floor Assessment:

Sum of the axial load obtained from G + nQ loading: 382500 N
Total number of columns on the floor: 8
Total column area on the floor: (300*300*8) = 720000 mm^2
Total axial compressive stress: (382500/720000) = 0.531 Mpa
Average axial compressive stress: (0.531/8) = 0.066 Mpa
Floor shear force limit value: 0.35
The sum of the shear forces of the elements exceeding the risk limit: 269.121 kN
Total floor shear force: 269.121 kN
269.121/269.121 = 1 > 0.35 **The floor is risky**.

3. CONCLUSION

This study aimed to examine and determine the risk status of buildings constructed before 2000 in the Siverek district of Şanlıurfa province. A reinforced concrete structure with two stories was designed for this purpose, and its risk assessment was performed. The existing concrete strength and reinforcement status of the designed building is considerably beyond the scope of the current regulation and insufficient. The risk assessment of the building examined in this study was carried out in accordance with the principles of low-rise reinforced concrete structures established in RYTEIE (2019). The structure is made up of 16 columns and is supported by a frame system. The risk of each of these vertical elements was assessed, risk analysis was performed inside each floor, and the risk status of the building was established. The current version (published in 2019) of RDRB, which entered into force in 2013, will enable a more comprehensive examination of the risk structure analysis by making various additions to the current version of the Earthquake Hazard Maps of Turkey. It is remarkable that the features of our country's building stock are identical to those found in the literature and field studies. As a result, it is suggested that the building stock built before and after 2000 be inspected in accordance with the recent regulations.

REFERENCES

[1] Yön, B., Onat, O., Öncü, M. E., and Karaşin, A. Failures of masonry dwelling triggered by East Anatolian Fault earthquakes in Turkey. Soil Dynamics and Earthquake Engineering, 133, 106126. 2020.
[2] A. Ünal. Reinforcement of reinforced concrete frames not designed according to TDY 2007 with a toothed shear wall. Selcuk University Graduate School of Natural and Applied Sciences. Konya. 2012.
[3] TMMOB Chamber of Geological Engineers (jmo.org.tr)
[4] Ulutas H. Comparison of DBYBHY (2007) and TBDY (2018) Earthquake Regulations in terms of Section Damage Limits. European Journal of Science and Technology. vol 17. pp. 351-359. 2019.
[5] Ayhan, Ersin, Gültekin AKTAŞ, and Abdulhalim KARAŞİN. "Evaluation of some buildings in Siirt according to the risky building detection regulation." Dicle University Engineering Faculty Journal of Engineering 12.1. 89-98. 2021.
[6] Turkoglu, Akin. and Meydanli Atalay. H., "Determination of Earthquake Safety of a Historic Masonry Building in the Scope of TBDY-2018 and RYTEIE-2019." Düzce University Journal of Science and Technology 10.4: 1926-1938. 2022.
[7] Alicioglu, M. B. Earthquake Risk of Existing Reinforced Concrete Buildings in the Center of Manisa. Journal of Disaster and Risk, 5(1), 138-150. 2022.
[8] Türkel, Y. E., and Tekeli, H. Earthquake risk assessment of residential reinforced concrete buildings. Journal of Polytechnic, 21(3), 669-680. 2018.
[9] S. Altın Karayahshi. Comparison of Existing Building Evaluation and Risky Building Evaluation in Public Buildings. Master Thesis. Celal Bayar University Institute of Science and Technology. Manisa. 2016.
[10] Z. Korkmaz. Comparison of the "Japanese Seismic Method" and the "Detection Principles of Risky Structures 2013" Regulation in Determining the Earthquake Performance of Buildings. Master Thesis. Maltepe University Institute of Science and Technology, Istanbul. 2017.
[11] Okuyucu, D., Savaş, G. K., Gedik, B., Şuşarlıoğlu, M. F., and Tarık, K. A. Determination of regional earthquake risk distribution of buildings by street scanning method: Erzurum–Yenişehir sample. Fırat University Journal of Engineering Sciences, 30(1), 219-231. 2018.
[12] E. Ekinci. Urban Transformation Studies and Cost Analysis for Risky Building Stock in Turkey: A Case Study. Master Thesis. Gazi University Institute of Science and Technology. Ankara. 2018.
[13] S. Can. Evaluation of Risky Buildings by Earthquake Safety Screening Method. Master Thesis. Istanbul Technical University, Institute of Science and Technology. Istanbul. 2019.
[14] Işık, E. and Tozlu, Z., "Calculating Building Performance Score Using Different Variables." Bitlis Eren University Journal of Science 4.2. 161-172. 2015.
[15] Hacımustafaoglu. S.F. Altan. M.F. Naim. S. Determination of Risk Situations of Risky Buildings by Observational Analysis. Aurum Journal of Engineering Systems and Architecture. vol. 5.1 pp. 109-118.
[16] Gürbüz. A. and Tekin. M. Determination of Regional Earthquake Risk Distribution of Existing Buildings by Performance Ranking Method. Celal Bayar University Journal of Science. vol. 11.1 pp. 37-48. 2015.
[17] Işık. E. Calculation of the Performance Score of a Damaged Reinforced Concrete Building. International Anatolia Academic Online Journal. vol. 3, 2, pp. 47-52. 2015.
[18] Işık. E. and Dusty. Z. Calculation of Building Performance Score Using Different Variables. Bitlis Eren University Journal of Science. vol. 4.2 pp. 161-172. 2015.

BIOGRAPHIES

İsmail Ümit ÇIKMAN born in 1994 in Şanlıurfa, Siverek. He graduated from Harran University, Department of Civil Engineering in 2017. Later, he completed his master's degree in Dicle University, engineering faculty, civil engineering department, building department in 2020. Currently, he continues his doctorate education in the Department of Materials at Bartın University, Department of Civil Engineering. In addition, after working as an Instructor in Afyon Kocatepe University, Faculty of Engineering, Civil Engineering, he is now working as an Instructor in Dicle University Technical Sciences Vocational School, Construction Department, Construction Technology Program. His fields of study are earthquake resistant building design, examination of risky structures and building materials.

Mehmet Emin ÖNCÜ received the B.Sc. degree in Civil Engineering in 1994 from Harran University. He received his M.Sc degree in Civil Engineering in 2000 from Atatürk University, and his Ph.D. degree in Civil Engineering in 2008 from Fırat University. Currently, he works as Associate Professor at Dicle University, Diyarbakır, Turkey. His research focuses on nonlinear analysis, performance-based seismic design and evaluation, risky structures, historical structures, repair and retrofitting of structures.

Şermin KOÇYİĞİT born 1978, received her Msc and PhD at the University of Firat, Elazığ, Turkey, in 2004 and 2016, respectively, while working in the institute of science and technology, building education department. At present, she is employed at the University of Dicle. Her fields of interests include materials science, hydraulic, risky structures, building materials.